Computers and Concrete, Vol. 8, No. 2 (2011) 125-142
DOI: http://dx.doi.org/10.12989/cac.2011.8.2.125

Mesoscale simulation of chloride diffusion in concrete considering the binding capacity and concentration dependence

Licheng Wang*[1] and Tamon Ueda[2]

[1]*State Key Laboratory of Coastal and Offshore Engineering, Dalian University of Technology Dalian 116024, China*
[2]*Faculty of Engineering, Hokkaido University, Sapporo 060-8628, Japan*

(Received July 6, 2009, Accepted August 9, 2010)

Abstract. In the present paper, a numerical simulation method based on mesoscopic composite structure of concrete, the truss network model, is developed to evaluate the diffusivity of concrete in order to account for the microstructure of concrete, the binding effect of chloride ions and the chloride concentration dependence. In the model, concrete is described as a three-phase composite, consisting of mortar, coarse aggregates and the interfacial transition zones (ITZs) between them. The advantage of the current model is that it can easily represent the movement of mass (e.g. water or chloride ions) through ITZs or the potential cracks within concrete. An analytical method to estimate the chloride diffusivity of mortar and ITZ, which are both treated as homogenious materials in the model, is introduced in terms of water-to-cement ratio (*w/c*) and sand volume fraction. Using the newly developed approaches, the effect of cracking of concrete on chloride diffusion is reflected by means of the similar process as that in the test. The results of calculation give close match with experimental observations. Furthermore, with consideration of the binding capacity of chloride ions to cement paste and the concentration dependence for diffusivity, the one-dimensional nonlinear diffusion equation is established, as well as its finite difference form in terms of the truss network model. A series of numerical analysises performed on the model find that the chloride diffusion is substantially influenced by the binding capacity and concentration dependence, which is same as that revealed in some experimental investigations. This indicates the necessity to take into account the binding capacity and chloride concentration dependence in the durability analysis and service life prediction of concrete structures.

Keywords: mesoscale simulation; chloride diffusion; binding capacity; concentration dependence; truss network model.

1. Introduction

For concrete structures exposed to seawater or de-icing salt, the chloride-induced corrosion of reinforcing steel has become one of the major causes of deterioration. It is generally recognized that when the chloride content at the level of reinforcement reaches a critical value, the corrosion of steel may begin to initiate. Therefore, it is of great significance to accurately investigate the transport properties of concrete, e.g. the diffusivity of aggressive ions or gases, in order to predict the initiation time of corrosion of reinforcements and to estimate the service life of concrete structures.

* Corresponding author, Associate Professor, Ph.D., E-mail: wanglicheng2000@163.com

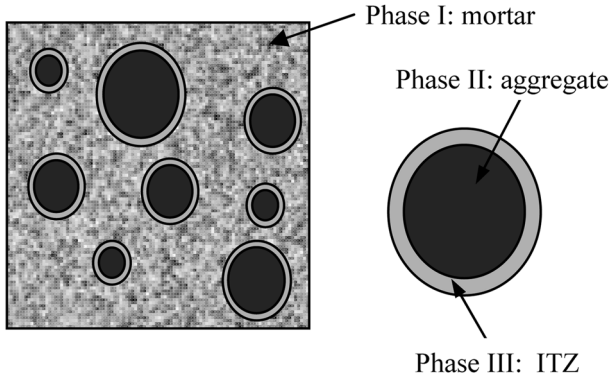

Fig. 1 The three-phase structure of concrete on mesoscale

On mesoscale, concrete is commonly supposed as a heterogeneous material. As a result, from the viewpoint of modeling, it is often treated as a three-phase composite material in which aggregates are embedded in a matrix of hardened cement paste, and the interfacial transition zones (ITZs) are assumed on the interface between aggregate particles and the surrounding cement paste (Oh and Jang 2004, Yang 2003, Caré and Hervé 2004). For the generally used aggregates, i.e. the fine and coarse aggregates, they are non-permeable (Oh and Jang 2004, Garboczi and Bentz 1998). In addition, recent research shows that the ITZs between cement paste and aggregates, especially coarse aggregates, can more effectively explain the phenomena of chloride diffusion (Takewaka *et al*. 2003). Regarding the high amount and relatively smaller size of fine aggregates, in the present study, only coarse aggregates are regarded as the non-sorptive inclusions. But the mortar, filled with fine aggregates, is supposed as a nominal homogeneous material in order to reduce the calculation work. The three-phase composite structure of concrete proposed in this study is schematically shown in Fig. 1.

When chloride ions penetrate into concrete, it has been verified that some of them will be chemically and physically bound to the hydrated products of cement and their surfaces in concrete (Martín-Pérez *et al*. 2000, Mien *et al*. 2009). This behavior is called chloride binding capacity of concrete, which has been quantitively defined as the slope of the binding isotherm (Tang and Nilsson 1993). As a result, chloride in concrete structures is commonly classified into free and bound chloride and only the free chloride is supposed to be responsible for the initiating corrosion process of the reinforcement because they can penetrate freely through the concrete cover to reach the reinforcing steel layer. It has been found that the concrete binding capacity has an important effect on the rate of chloride ions transport in concrete and on the corrosion initiation of the steel reinforcement due to the reduction of the amount of chloride ions available to initiate the deterioration process (Martín-Pérez *et al*. 2000, Boddy *et al*. 1999, Nillson *et al*. 1996). In addition, the concentration dependence of diffusivity on free chloride diffusion has also been investigated and proved. In concrete, the mortar, but not the coarse aggregate, is apparently the major composition to which chloride ions are bound (Tang and Nilsson 1993), therefore, the mesocale modeling techniques offer a promising solution to really represent the binding effect.

The purpose of this paper is to develop a numerical method on mesoscale to investigate the diffusivity of concrete in order to account for the microstructure of concrete (i.e. the ITZs and cracks) and to take into consideration the binding effect of chloride ions and the chloride

concentration dependence. In terms of this model, it will be helpful to simulate the diffusion process of chloride ions in concrete for more accurate analysis and better prediction of the durability and service life of concrete structures.

2. Truss network model

2.1 Construction of truss network model

In this paper, the Voronoi diagram is used as the meshing tool for the concrete specimen considering its advantages in simulating the crack formation and propagation, as well as the crack width, which are necessarily needed for predicting the deterioration performance and durability of concrete structures (Nagai *et al*. 2004, Nakamura *et al*. 2006). The random characteristic of geometry of the elements meshed by Voronoi diagrams makes it possible not to prescribe the locations and directions of crack propagation because cracks are doomed to initiate and propagate along the elements boundaries. This means that the adaptive re-meshing is not needed (Bolander and Le 1999). Fig. 2(a) shows the Voronoi diagram after meshing a concrete specimen on the level of mesoscale.

The truss network model is subsequently established based on the Voronoi diagram. Each of the Voronoi elements is linked by truss elements with nodes at the centres of Voronoi elements and the intermediate points on Voronoi element boundaries (see Fig. 2(b)). This is a refined approach of truss network model proposed by Nakamura *et al*. (2006), in which only the Voronoi nuclei are linked to generate a truss element (Bolander and Berton 2004). The advantages of this modification, i.e. connecting the intermdiate points on Voronoi element boundaries, can easily represent the movement of mass (e.g. water or chloride ions) through ITZs or the potential cracks. As a result, the substance transport in a two-dimensional area is simplified to a set of one-dimensional problems in the network, not only suitable for the uncracked but also for the cracked concrete. For uncracked concrete, the cross sectional area and diffusivity of a truss element are set according to the following rules: for truss elements within aggregate, both are assumed as 0; for truss elements within mortar, the cross sectional areas are given according to the corresponding Voronoi element area. On the Voronoi element boundaries, there are two kinds of truss elements. The first kind is for

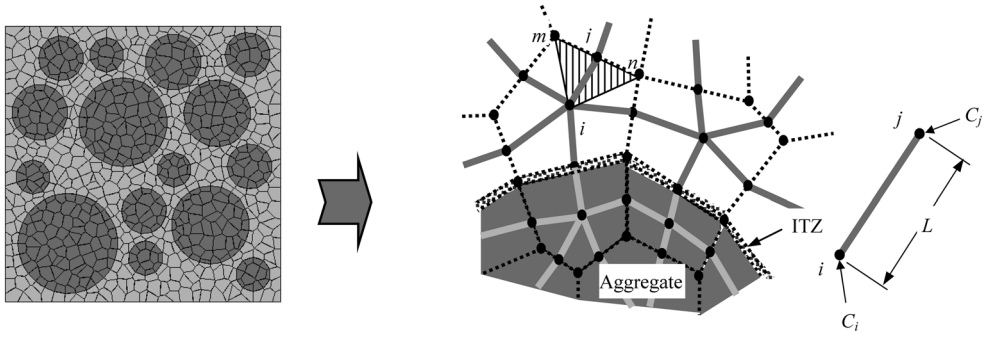

(a) Voronoi diagram (b) Construction of truss network

Fig. 2 Construction of the truss network model

those on the interfaces of two mortar Voronoi elements, and their cross sectional areas are assumed as 0 assuming no mass transfer occurrence. The second kind is for those just between aggregate and mortars, i.e. in ITZs, and their cross sectional areas and diffusivity have been studied and determined through experimental method and numerical analysis technique.

2.2 Governing equation of chloride diffusion

Usually the Fick's second law is used as the governing equation for chloride diffusion process in concrete. When the free chloride concentration is substituted for the total chloride concentration, the governing equation is given as follows

$$\frac{\partial C_f}{\partial t} = \frac{\partial C_f}{\partial C_t}\frac{\partial}{\partial x}\left(D_{cl}\frac{\partial C_f}{\partial x}\right) \tag{1}$$

where C_t is the total chloride concentration, in grams of total chloride per gram of concrete (g/g); C_f is the free chloride concentration, in grams of free chloride per gram of concrete (g/g); D_{cl} is chloride diffusion coefficient (mm^2/day); t is time in days; x is the distance from the exposed surface of concrete in mm.

The two material parameters, the binding capacity of cement paste and the concentration dependence of chloride diffusivity, have been studied and given in previous literatures (Xi and Bazant 1999, Ababneh *et al*. 2003), which will be discussed in the following subsections.

2.3 Concentration dependence

The chloride diffusion coefficient is somehow influenced by the free chloride concentration, i.e. the diffusivity decreases with the increase of C_f (Xi and Bazant 1999). This concentration dependent relationship can be expressed as

$$D_{ion} = D'[1 - k_{ion}(C_f)^m] \tag{2}$$

in which D_{ion} and D' are the diffusion coefficient when considering the concentration dependence and not considering the concentration dependence respectively; $D' = RT\Lambda_0/F^2|Z_{ion}|$, where F is the Faraday constant; R is the gas constant; T is temperature; Λ_0 is the reference conductance; Z_{ion} is the valency of the ion; C_f is defined in terms of the weight of concrete; m is a constant, usually taken a typical value of 0.5 (Atkins 2001). And, $k_{ion} = k_c/\Lambda_0$, in which k_c is the Kohlrausch coefficient depending on the nature of the specific salt in solution. According to the computations and comparisons with test results, it was estimated as $k_{ion}=\sqrt{70}$ (Xi and Bazant 1999).

2.4 Chloride binding capacity

As defined, the total chloride concentration is the sum of bound chloride concentration, C_b, and free chloride concentration, C_f, meaning

$$C_t = C_b + C_f \tag{3}$$

The chloride binding capacity is defined as follows

$$\frac{\partial C_f}{\partial C_t} = \frac{1}{\dfrac{\partial C_t}{\partial C_f}} = \frac{1}{\dfrac{\partial (C_f + C_b)}{\partial C_f}} = \frac{1}{1 + \dfrac{\partial C_b}{\partial C_f}} \tag{4}$$

Generally, the ratio $\partial C_b/\partial C_f$ can be determined experimentally. Based on the relationship between the C_f and C_b established by Freundlich isotherm (Tang and Nilson 1993, Delagrave *et al.* 1996), a prediction model for the binding capacity has been developed (Xi and Bazant 1999).

$$\frac{\partial C_f}{\partial C_t} = \frac{1}{1 + \dfrac{A 10^B \beta_{gel}}{35450 \beta_{sol}} \left(\dfrac{C_f}{35.45 \beta_{sol}} \right)^{A-1}} \tag{5}$$

in which A and B are two material constants, determined as 0.3788 and 1.14 for ordinary portland cement (OPC), respectively (Tang and Nilson 1993); β_{sol} is the ratio of pore solution to concrete, in liters of the pore solution per gram of the concrete (L/g); β_{gel} is the ratio of C-S-H gel to concrete, in grams of C-S-H gel per gram of concrete (g/g). The two parameters, β_{sol} and β_{gel} can be determined by the water-to-cement ratio (w/c) and mix proportion of concrete.

Parameter β_{sol} From the definition of β_{sol}, it yields

$$\beta_{sol} = \frac{V_{sol}}{W_{conc}} \tag{6}$$

where V_{sol} is the volume of the pore solution (L); W_{conc} is the weight of concrete (g). Due to the relatively small porosity of aggregates, the volume of the pore solution can be represented by that of the paste cement.

The Powers's model has been widely used to quantify the composite structure of hardened Portland cement paste, because the fractional volumes of all major constituents in the physical structure of room temperature cured Portland cement paste can be estimated from information on w/c and degree of hydration of the cement (Hansen 1986). Moreover, it is pointed out that the total porosity of a hydrated cement paste is the sum of the gel porosity and capillary porosity (Jennings and Tennis 1994). The fractional volume of gel pores is expressed as

$$\phi_{gel} = \frac{0.19 \alpha}{(w/c) + V_{cem}} \tag{7}$$

where V_{cem} is the specific volume of cement in cm^3 per gram. For the common OPC, V_{cem} may be assumed as 0.32 cm^3 per gram; α is the ultimate degree of hydration, which is defined as the ratio between the amount of cement that has become hydrated finally and the original cement amount. The ultimate degree of hydration α is empirically expressed as the function of w/c (Oh and Jang 2004)

$$\alpha = 1 - \exp(-3.15(w/c)) \tag{8}$$

The capillary porosity is estimated by the following equation

$$\phi_{cap} = \frac{(w/c) - 0.36 \alpha}{(w/c) + V_{cem}} \tag{9}$$

Thus, the total porosity can be written as

$$\phi_{por} = \phi_{cap} + \phi_{gel} = \frac{(w/c) - 0.22\alpha}{(w/c) + V_{cem}} \tag{10}$$

For a mixture proportion of concrete with cement of W_{cem}, weight of cement per m^3 concrete and with water of W_{wat}, weight of water per m^3 concrete respectively, the volume of hydrated cement paste V_{cp} of a W_{conc} bulk concrete can be formulated as

$$V_{cp} = (W_{cem}V_{cem} + W_{wat}V_d) \times \frac{W_{conc}}{\rho_{conc}} \tag{11}$$

in which V_d is the specific volume of mixing water, generally equaling 1 cm^3 per gram; ρ_{conc} is the density of concrete, approximately taken as 2.3 g/cm^3; V_{cp} is in cm^3. By combining Eq. (6) to Eq. (11), it yields

$$\beta_{sol} = \frac{V_{cp} \times \phi_{por}}{1000 \times W_{conc}} (W_{cem}V_{cem} + W_{wat}V_d) \frac{\phi_{por}}{1000 \times \rho_{conc}} = \frac{(W_{cem}V_{cem} + W_{wat}V_d)((w/c) - 0.17\alpha)}{1000 \times \rho_{conc}((w/c) + V_{cem})} \tag{12}$$

Parameter β_{gel} As defined, β_{gel} can be expressed as

$$\beta_{gel} = \frac{W_{gel}}{W_{conc}} \tag{13}$$

The fractional volume of C-S-H gel of the hydrated cement paste has obtained as

$$\gamma_{gel} = \frac{0.68\alpha}{(w/c) + V_{cem}} \tag{14}$$

So the weight of C-S-H gel of a W_{conc} bulk concrete can be written as

$$W_{gel} = \rho_{gel}\gamma_{gel}V_{cp} \tag{15}$$

where ρ_{gel} is the density of C-S-H gel, usually ρ_{gel} =2.34 g/cm^3. And then

$$\beta_{gel} = \frac{\rho_{gel}\gamma_{gel}V_{cp}}{W_{conc}} = \frac{0.68\rho_{gel}\alpha(W_{cem}V_{cem} + W_{wat}V_d)}{\rho_{conc}((w/c) + V_{cem})} \tag{16}$$

3. Analytical method for the diffusivity of mortar and ITZs

3.1 Diffusivity of cement paste

The diffusivity of cement paste can be estimated assuming that cement paste is regarded as a two-phase composite, the capillary pores and the solid particles. The model proposed by Oh and Jang (2004) is used in this study because it can cover the entire capillary porosity range, which is expressed as

$$\frac{D_p}{D_0} = \left(m_\phi + \sqrt{m_\phi^2 + \frac{\phi_c}{1 - \phi_c}\left(\frac{D_s}{D_0}\right)^{1/n}} \right)^n \tag{17}$$

in which D_p are the diffusivity of cement paste; D_0 is the ionic diffusivity in bulk fluid, taken as 2.032×10^{-9} m^2/s at 25°C for chloride ions in water; D_s is the diffusivity of the solid phase, denoting the diffusivity when the capillary porosity equals to zero; ϕ_c is the critical porosity that the pore

network first percolates, which means that the diffusion can occur only over the percolation threshold; n is the percolation exponent constant. In this equation, m_ϕ is written as

$$m_\phi = \frac{1}{2}\left[\left(\frac{D_s}{D_0}\right)^{1/n} + \frac{\phi_{cap}}{1-\phi_c}\left(1-\left(\frac{D_s}{D_0}\right)^{1/n}\right) - \frac{\phi_c}{1-\phi_c}\right] \tag{18}$$

where ϕ_{cap} is the capillary porosity.

It was found that the values for n and D_s/D_0 obtained for the test dada are $n \approx 2.7$ and $D_s/D_0 \approx 2.0\times10^{-4}$ for OPC. In addition, the critical porosity ϕ_c is proposed as 0.18 by Bentz and Garboczi (1991) and the capillary porosity can be estimated by Eq. (9).

3.2 Diffusivity of mortar and ITZs - the effect of addition of aggregates

Generally speaking, the presence of aggregates in a hydrated cement paste matrix has two opposite effects on the transport properties (Delagrave *et al.* 1997, Yoon 2009). First, the addition of solid particles leads to an increase in the tortuosity of matrix, so the chloride ions have to move around the solid particles. This implies that tortuosity (redirecting) effects reduce the transport speed. Second, the presence of porous and connected ITZs probably contributes to facilitating the movement of ions. Therefore, in order to investigate the effect of aggregate content and ITZs on the transport properties, the mortar can also be regarded as a three-phase composite material. Based on this assumption, the diffusivity of mortar has been proposed as (Oh and Jang 2004)

$$\frac{D_m}{D_p} = 1 + \frac{V_a}{\dfrac{1}{2(D_{\mathrm{ITZ}}/D_p)\varepsilon - 1} + \dfrac{1-V_a}{3}} \tag{19}$$

in which D_m and D_{ITZ} are the diffusivity of mortar and ITZ, respectively; V_a is the volume fraction of aggregate particles; ε is the ratio of the ITZ thickness and the radius of aggregate particle, which may be approximated by considering the mean radius of aggregate particles. Additionally, D_{ITZ} can also be estimated by Eq. (17) assuming $\phi_{ITZ} = 1.5\phi_{cap}$ (Oh and Jang 2004). From the above analysis,

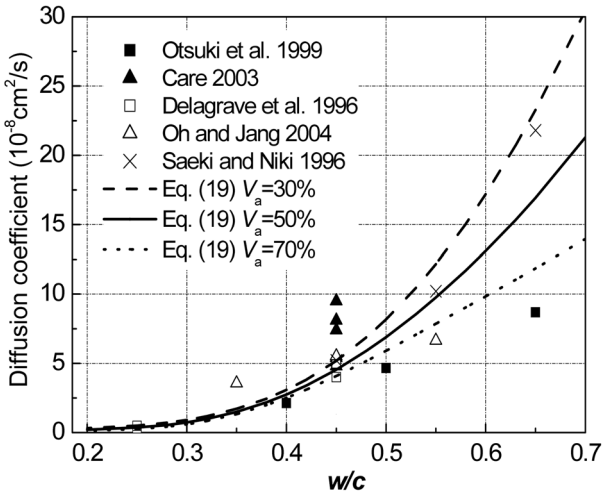

Fig. 3 Effect of w/c and aggregates volume fractions on the diffusivity of mortar

one can see that w/c is the dominating factor on the diffusivity of mortar due to its crucial importance to the capillary porosity of cement paste. Fig. 3 shows the effect of w/c on chloride diffusion coefficient of mortar. It can be seen that with the increase of w/c, the diffusion coefficient increases due to the increase of capillary porosity of cement paste. Some available experimental data on chloride diffusion coefficient of mortar are also depicted in Fig. 3 to verify Eq. (19). One can see that, although the mixtures in those experiments are quite different from each other, the model represented by Eq. (19) can show a relatively good correlation with experimental data.

4. Numerical solution

4.1 The differential governing equation

As both the binding capacity and diffusion coefficient are dependent on the free chloride concentration, the governing equation, represented by Eq. (1), can be written in a simple form as follows

$$\frac{\partial C_f}{\partial t} = \frac{1}{u(C_f)} \frac{\partial}{\partial x}\left(v(C_f) \frac{\partial C_f}{\partial x} \right) \tag{20}$$

The formation of $u(C_f)$ is the denominator of the expression on the right hand of Eq. (4) and $v(C_f)$ can be represented by Eq. (2). Although $v(C_f)$ in Eq. (20) can be regarded as an apparent diffusion coefficient, it is worth noting that $v(C_f)$ is a function of the free chloride concentration instead of being a constant.

Thus, Eq. (20) can be written as

$$\frac{u(C_f)}{v(C_f)} \frac{\partial C_f}{\partial t} = \frac{1}{v(C_f)} \frac{\partial v}{\partial C_f} \cdot \left(\frac{\partial C_f}{\partial x} \right)^2 + \frac{\partial^2 C_f}{\partial x^2} \tag{21}$$

4.2 Spatial dispersion by the gallerkin weighted residual method

The nonlinearity of differential governing equation due to concentration dependence of the diffusion coefficient and binding capacity makes analytical solution for Eq. (21) impossible. Therefore, in the present study, the Gallerkin weighted residual method will be used to disperse Eq. (21) numerically, and then the numerical method will be applied to the truss network model.

To a 1-dimentional line element with length of l, if the values at two end points, x_i and x_j, are respectively assumed as $F(C_f)_i$ and $F(C_f)_j$ for any function of $F(C_f)$, the approximate expression of $F(C_f)$ along the element ij can be linearly described as

$$F(C_f) = \frac{x_j - x}{l} F(C_f)_i + \frac{x - x_i}{l} F(C_f)_j \tag{22}$$

Here, $F(C_f)$ can be any expression of the free chloride concentration C_f. For simplicity, one can set $g_i = \frac{x_j - x}{l}$ and $g_j = \frac{x - x_i}{l}$, which are regarded as the weighted residual functions. Subsequently, according to the Gallerkin method, the following two equations can be obtained

$$\tilde{R}_i = A\int_{x_i}^{x_j} g_i\left[\frac{\partial^2 C_f}{\partial x^2}+\frac{1}{v(C_f)}\frac{\partial v}{\partial C_f}\left(\frac{\partial C_f}{\partial x}\right)^2-\frac{u(C_f)}{v(C_f)}\frac{\partial C_f}{\partial t}\right]dx = I_1+I_2+I_3 = 0 \tag{23}$$

$$\tilde{R}_j = A\int_{x_i}^{x_j} g_j\left[\frac{\partial^2 C_f}{\partial x^2}+\frac{1}{v(C_f)}\frac{\partial v}{\partial C_f}\left(\frac{\partial C_f}{\partial x}\right)^2-\frac{u(C_f)}{v(C_f)}\frac{\partial C_f}{\partial t}\right]dx = J_1+J_2+J_3 = 0 \tag{24}$$

in which A is the sectional area of the 1-dimentional line element. The integrals of each part in the above two equations can be derived seperately. The procedure is described fully in the Appendix. Then Eqs. (23) and (24) can be written in the form of simultaneous equations

$$\begin{Bmatrix}\tilde{R}_i\\ \tilde{R}_j\end{Bmatrix} = \begin{Bmatrix}-A\dfrac{\partial C_f}{\partial x}\Big|_{x=x_i}\\ A\dfrac{\partial C_f}{\partial x}\Big|_{x=x_j}\end{Bmatrix} - \frac{A}{l}\begin{bmatrix}1+\frac{1}{2}P & -1-\frac{1}{2}P\\ -1+\frac{1}{2}P & 1-\frac{1}{2}P\end{bmatrix}\begin{Bmatrix}C_{fi}\\ C_{fj}\end{Bmatrix} - \frac{lA}{6}\begin{bmatrix}2Q & R\\ Q & 2R\end{bmatrix}\begin{Bmatrix}\dfrac{\partial C_{fi}}{\partial t}\\ \dfrac{\partial C_{fj}}{\partial t}\end{Bmatrix} = \begin{Bmatrix}0\\0\end{Bmatrix} \tag{25}$$

where, $P = \ln\dfrac{v(C_{fj})}{v(C_{fi})}$, $Q = \dfrac{u(C_{fi})}{v(C_{fi})}$, $R = \dfrac{u(C_{fj})}{v(C_{fj})}$.

Since Eq. (25) is in the equational form, it can also be written as

$$\begin{Bmatrix}A\dfrac{\partial C_f}{\partial x}\Big|_{x=x_i}\\ -A\dfrac{\partial C_f}{\partial x}\Big|_{x=x_j}\end{Bmatrix} + \frac{A}{l}\begin{bmatrix}1+\frac{1}{2}P & -1-\frac{1}{2}P\\ -1+\frac{1}{2}P & 1-\frac{1}{2}P\end{bmatrix}\begin{Bmatrix}C_{fi}\\ C_{fj}\end{Bmatrix} + \frac{lA}{6}\begin{bmatrix}2Q & R\\ Q & 2R\end{bmatrix}\begin{Bmatrix}\dfrac{\partial C_{fi}}{\partial t}\\ \dfrac{\partial C_{fj}}{\partial t}\end{Bmatrix} = \begin{Bmatrix}0\\0\end{Bmatrix} \tag{26}$$

If only the diffusion process is used to account for the chloride ions penetrating into concrete, the following initial condition, $C_f = C_0$, $x \geq 0$, $t = 0$, and boundary condition, $C_f = C_s$, $x = 0$, $t > 0$, are applied to solve the above equation. Here, C_0 is the initial free chloride concentration in concrete; C_s is the surface chloride concentration exposed to air or water environment.

Further, Eq. (26) can be simplified as

$$\{f\}+[k]\{C_f\}+[c]\left\{\frac{\partial C_f}{\partial t}\right\} = \{0\} \tag{27}$$

This is the finite element equation for a single truss element. If all the truss elements in a meshed area are integrated, the global finite equation can be formed as

$$\{F\}+[K]\{C_f\}+[C]\left\{\frac{\partial C_f}{\partial t}\right\} = \{0\} \tag{28}$$

4.3 Solution method

In this paper, the Crank-Nicholson method is used to numerically solve the above equation. By introducing the discrete time step Δt, one can have

$$\left\{C_f\left(t+\frac{\Delta t}{2}\right)\right\}=\frac{1}{2}(\{C_f(t+\Delta t)\}+\{C_f(t)\}) \tag{29}$$

Then the differential formation at time $(t + \Delta t/2)$ in time space can be expressed as

$$\left\{\frac{\partial}{\partial t}C_f\left(t+\frac{\Delta t}{2}\right)\right\}=\frac{\{C_f(t+\Delta t)\}-\{C_i(t)\}}{\Delta t} \tag{30}$$

By substituting Eqs. (29) and (30) into Eq. (28) and adjusting, one can have the basic formation for the discrete time calculation process

$$\left(\frac{1}{2}[K]+\frac{1}{\Delta t}[C]\right)\{C_f(t+\Delta t)\}=\left(-\frac{1}{2}[K]+\frac{1}{\Delta t}[C]\right)\{C_f(t)\}-\{F\} \tag{31}$$

It should be noted that in Eq. (31), because the matrices $[K]$ and $[C]$ are both dependent on the free chloride concentration, their values may be approximately estimated based on the free chloride concentration after the former step. It implies that an iterative process must be adopted until a given convergence criterion is reached. Here, the convergence of computation is judged when the square root of the sum-of-squared-error btween the current and former steps becomes less than 10^{-5}.

5. Results and discussion

5.1 Chloride diffusion in cracked concrete

In the experiment by Olga and Doug Hooton (2003), a transecting, parallel-wall crack with approximately

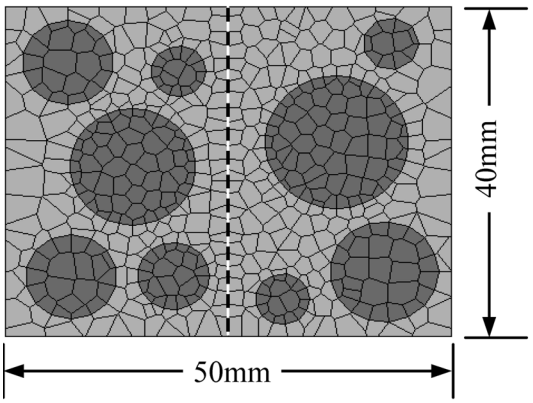

Fig. 4 Numerical model of the cracked concrete (dotted line indicating the position of crack)

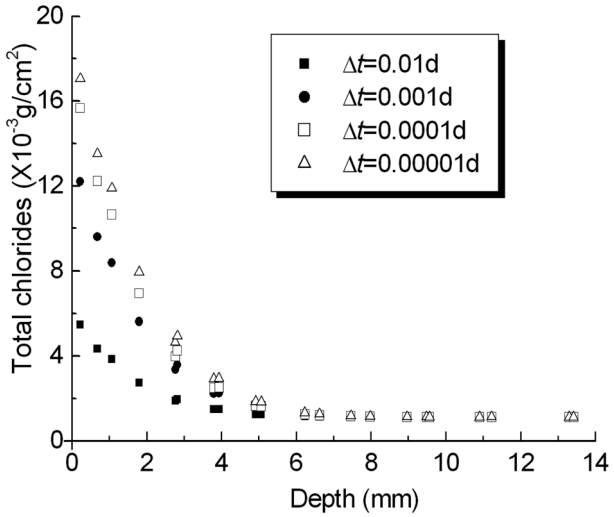

Fig. 5 Effect of discrete time step Δt on the chloride profiles perpendicular to the crack surface (D_{cr} = 10000 mm^2/h, w_{cr} = 90 μm)

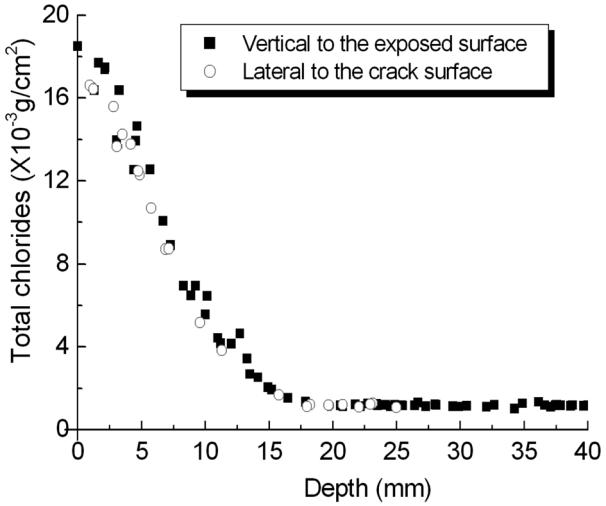

Fig. 6 Chloride profiles vertical to the exposed surface and vertical to the crack wall

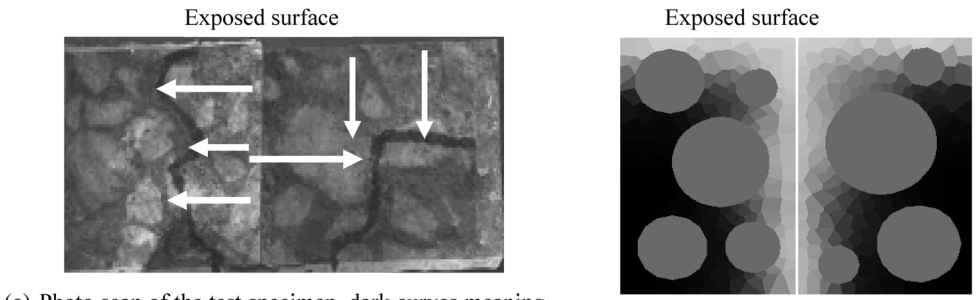

(a) Photo scan of the test specimen, dark curves meaning the diffusion depth (Olga & Doug Hooton 2003)

(b) Numerical analysis results

Fig. 7 Depth of chloride penetration in cracked concrete with single parallel-wall crack

constant width was induced in the sample concrete. In the current study, one example in their test with crack width (w_{cr}) of 90 μm is selected and the chloride diffusion coefficient through crack D_{cr} is set as 10000 mm^2/h by a series of fitting analysises of the test data from Ismail *et al*. (2004). The specimen after numerically discreted on mesoscale is shown in Fig. 4 by arranging the crack in the middle of the sample. The exposed time of the sample to chloride solution is 40 days. A sensitivity analysis is done in order to determine the appropriate discrete time step Δt as provided in Fig. 5. It is observed that when the time interval is less than 0.00001d, the chloride profiles perpendicular to the crack surface will become stable, therefore in the study of this paper, Δt = 0.00001d.

Both the chloride concentration profiles along depth of the specimen and vertical to the crack wall surface are recorded and presented in Fig. 6, also schematically shown in Fig. 7. From Fig. 6, it can be seen that the two chloride profiles are quite close to each other leading to the same conclusion obtained by experiment (Olga and Doug Hooton 2003, Ismail *et al*. 2008) that the lateral diffusion of chlorides from the crack wall surface into the bulk concrete is uniform along the crack pathway. The chloride profile obtained by Ishida *et al*. (2009) for a cracked concrete by modeling analysis is shown in Fig. 8, which has the quite similar tendency with that in Fig. 7(b). The example here used

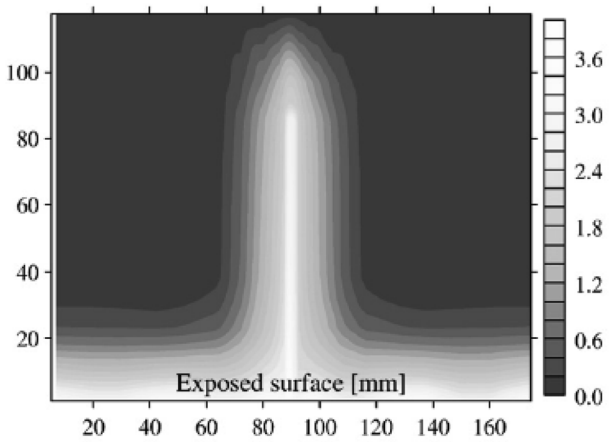

Fig. 8 Chloride profile in cracked concrete obtained by Ishida *et al*. (2009)

proved the feasibility and accuracy of the truss network model for a unique parallel-wall crack. As more knowledge on the D_{cr} of a single crack with any width are determined, the method can be extended to the case of multiple cracks (Wang *et al*. 2008).

5.2 Binding capacity and concentration dependece

The concrete specimen of numerical analysis is shown in Fig. 9. The *w/c* is 0.55 and the volume content of coarse aggregates is about 40%. The cement, sand and water contents are 316, 749 and 174 kg/m^3 respectively. These parameters are used to predict the parameters β_{sol} and β_{gel} by Eq. (12) and (16) respectively. Only the left side of the specimen is set to be exposed to the chloride source and all the other sides are supposed to be sealed without chlorides penetration. The chloride

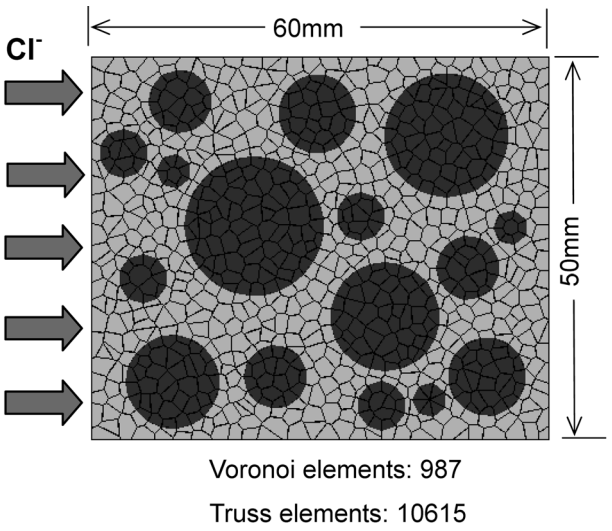

Fig. 9 The model and analysis conditions of the specimen

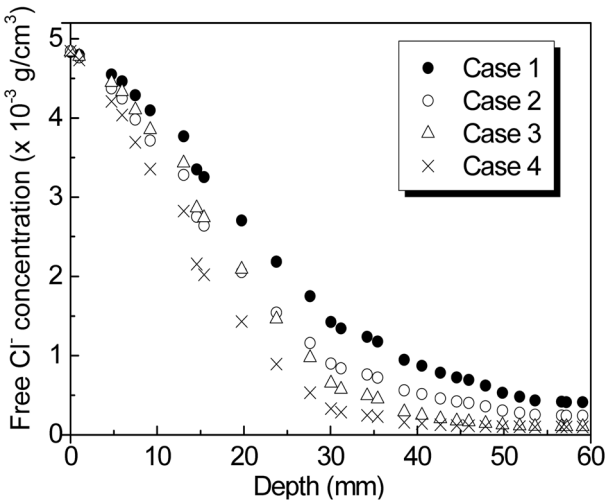

Fig. 10 Predicted chloride profiles after exposure of 600 days for the 4 cases

concentration is assumed as 4.86×10^{-3} g/cm^3 on the exposed boundary. This unit means chloride concentration is in grams of free chloride per cm^3 of concrete (Saeki and Niki 1996). When the density of concrete is taken as 2.3 g/cm^3, it will become as 2.11×10^{-3} g/g in grams of free chloride per gram of concrete.

To investigate the effect of binding capacity and chloride concentration dependence, in this section, the surface chloride concentration is looked as free chloride concentration, but the chloride ions penetrating process will be separated as 4 cases. Case 1 indicates that neither the binding capacity nor chloride concentration dependence are considered; case 2 means only taking into account the chloride concentration dependence; case 3 means only taking into account the binding capacity; case 4 means both the binding capacity and chloride concentration dependence are considered. The comparison of chloride profiles after 600 days of exposure resulting from the 4 cases is presented in Fig. 10. It can be found that the predicted profiles differ too much whether the binding capacity and concentration dependence are considered or not, which clearly indicates the necessity to take into account the binding capacity and chloride concentration dependence in the durability analysis and service life prediction.

Fig. 11 shows the chloride concentration varying with exposure time at some locations in the specimen. One can obviously observe that it will take much longer time to reach a given chloride concentration for a fixed depth. For example, if the critical chloride level is set as 1×10^{-3} g/cm^3, it will take about 120 day at a depth of 19.7 mm to reach it, but when both the binding capacity and concentration dependence are considered, the exposure time will be extended to 425 days.

In experimental studies of chloride penetration by immersion or exposure methods, usually the concrete specimens are cut into slices and then ground into powders to measure the chloride content. Obviously, the chloride concentration recorded by this process is the total chloride amount, including free chloride and bound chloride. It implies that the experimental findings must overestimate the effective chloride ions content in concrete because only the free chloride is responsible for the deterioration of concrete structures. Fig. 12 provides the comparison of chloride profiles between total, free and bound chloride concentration, which has the similar tendency as that observed in the experiment (De Vera *et al.* 2007). In Fig. 12, the bound chloride concentration is calculated by Eq. (3).

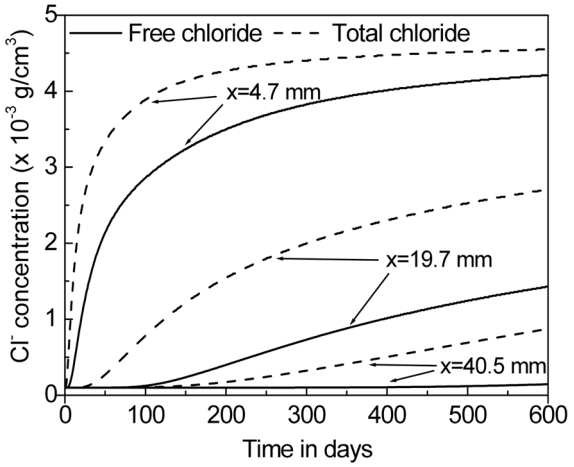

Fig. 11 Comparison of chloride profiles with and without consideration of binding capacity and concentration dependence

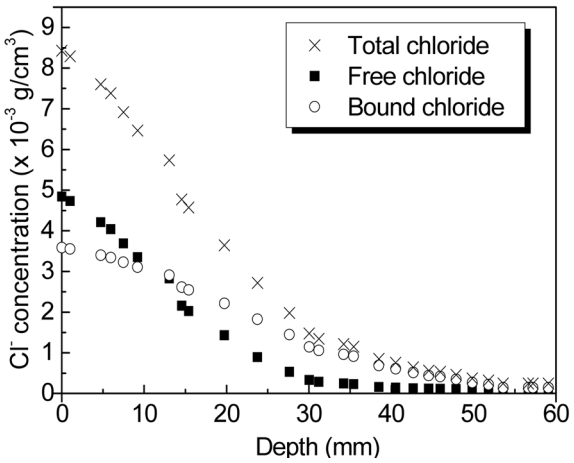

Fig. 12 Comparison of chloride concentration profiles between total, free and bound chlorides

6. Conclusions

A numerical approach on meso-scale, i.e. the truss network model is developed to successfully simulate the chloride diffusion within concrete, especially when the binding capacity of chloride ions with cement paste and the concentration dependence for diffusivity are taken into account. In the model, concrete is treated as a three-phase composite material, including the coarse aggregate, mortar and their interface. The another benefit of the currently developed method in this paper is that it can be used to represent the transport process of water or chloride ions through ITZs or the potential cracks in concrete.

An analytical approach to estimate the chloride diffusivity of mortar and ITZ, both of which are assumed as homogenious materials in the model respectively, is introduced in terms of the water-to-cement ratio and sand volume fraction. The one-dimensional nonlinear diffusion equation accounting for the binding capacity and the concentration dependence, as well as its finite differential form, which is applied to the truss network model on mesolevel, are built up by means of the Gallerkin method.

The effect of cracking can be conveniently implemented in the proposed model of concrete since the position of cracks has been predominated beforehand in the network. Based on the results of chloride diffusion in a transecting, parallel-wall cracked specimen, it is shown that cracks in concrete plays an important role in the diffusion property and accelerates the ingress speed of chloride ions. The results of calculation are quite close to the experimental observations.

The chloride diffusion is found to be substantially influenced by both the binding capacity and concentration dependence, which are illustrated by comparing chloride concentration profiles obtained from 4 cases respectively. The conclusion is that both the binding capacity and concentration dependence can reduce the diffusion rate of chloride ions. If they are ignored, the durability or the service life of concrete structures will be underestimated. Therefore, for more accurate prediction, it is necessary to consider their effects.

Acknowledgements

This study was supported by the Key Project of Chinese Ministry of Education (No. 109046) and the Scientific Research Foundation for the Returned Overseas Chinese Scholars, State Education Ministry. Also, financial support under the 21st Century COE Program 'Sustainable Metabolic System of Water and Waste for Area-based Society' of Hokkaido University and Center for Concrete Corea, Korea to the Yonsei University of Korea and the Grant-in-Aid for Scientific Research (A) No.19206048 from Japanese Government are gratefully acknowledged.

References

Ababneh, A., Benboudjema, F. and Xi, Y. (2003), "Chloride penetration in nonsaturated concrete", *J. Mater. Civil Eng.*, **15**(2), 183-191.

Atkins, P.W. (2001), *The elements of physical chemistry*, Oxford University Press.

Bolander, J.E. and Berton, S. (2004), "Simulation of shrinkage induced cracking in cement composite overlays", *Cement Concrete Comp.*, **26**(7), 861-871.

Bolander, J.E. and Le, B.D. (1999), "Modeling crack development in reinforced concrete structures under service loading", *Constr. Build. Mater.*, **13**(1-2), 23-31.

Boddy, A., Bentz, E., Thomas, M.D.A. and Hooton, R.D. (1999), "An overview and sensitivity study of a multimechanistic chloride transport model", *Cement Concrete Comp.*, **29**(6), 827-837.

Caré, S. (2003), "Influence of aggregates on chloride diffusion coefficient into mortar", *Cement Concrete Res.*, **33**(7), 1021-1028.

Caré, S. and Hervé, E. (2004), "Application of an n-phase model of the diffusion coefficient of chloride in mortar", *Transport. Porous Med.*, **56**(2), 119-135.

Delagrave, A., Bigs, J.P., Oliivier, J.P., Marchand, J. and Pigeon, M. (1997), "Influence of the interfacial zone on the chloride diffusivity of mortars", *Adv. Cement Based Mater.*, **5**(3-4), 86-91.

De Vera, G, Climent, M.A., Viqueira, E., Anton, C. and Andrade, C. (2007), "A test method for measuring chloride diffusion coefficients through partially saturated concrete. Part : The instantaneous plane source diffusion case with chloride binding consideration", *Cement Concrete Res.*, **37**(5), 714-724.

Garboczi, E.J. and Bentz, D.P. (1998), "Multiscale analytical/numerical theory of the diffusivity of concrete", *Adv. Cement Based Mater.*, **8**(2), 77-88.

Hansen, T.C. (1986), "Physical structure of hardened cement paste: a classical approach", *Mater. Struct.*, **19**(114), 423-436.

Ishida, T., Iqbal, P.O.N. and Anh, H.T.L. (2009), "Modeling of chloride diffusivity coupled with non-linear binding capacity in sound and cracked concrete", *Cement Concrete Res.*, **39**(10), 913-923.

Ismail, M., Toumi, A., Francois, R. and Gagne, R. (2004), "Effect of crack opening on the local diffusion of chloride in inert materials", *Cement Concrete Res.*, **34**(4), 711-716.

Ismail, M., Toumi, A., Francois, R. and Gagne, R. (2008), "Effect of crack opening on the local diffusion of chloride in cracked mortar samples", *Cement Concrete Res.*, **38**(8-9), 1106-1111.

Martín-Pérez, B., Zibara, H., Hooton, R.D. and Thomas, M.D.A. (2000), "A study of the effect of chloride binding on service life predictions", *Cement Concrete Res.*, **30**(8), 1215-1223.

Mien, T.V., Stitmannaithum, B. and Nawa, T. (2009), "Simulation of chloride penetration into concrete structures subjected to both cyclic flexural loads and tidal effects", *Comput. Concrete*, **6**(5), 421-435.

Nagai, K., Sato, Y. and Ueda, T. (2004), "Mesoscopic simulation of failure of mortar and concrete by 2D RBSM", *J. Adv. Concrete Tech.*, **2**(3), 359-374.

Nakamura, H., Srisoros, W., Yashiro, R. and Kunieda, M. (2006), "Time-dependent structural analysis considering mass transfer to evaluate deterioration process of RC structures", *J. Adv. Concrete Tech.*, **4**(1), 147-158.

Nilsson, L.O., Poulsen, E., Sandberg, P., Sùrensen, H.E. and Klinghoffer, O. (1996), *HETEK, chloride penetration into concrete, state-of-the-art, transport processes, corrosion initiation, test methods and prediction*

models, The Road Directorate, Copenhagen.
Oh, B.H. and Jang, S.Y. (2004), "Prediction of diffusivity of concrete based on simple analytic equations", *Cement Concrete Res.*, **34**(3), 463-480.
Otsuki, N., Hisada M., Otani, T. and Maruyama, T. (1999), "Theoretical evaluation of diffusion coefficient of chloride ion in mortar from mobility", *ACI Mat. J.*, **96**(6), 627-633.
Saeki, T. and Niki, H. (1996), "Migration of chloride ions in non-saturated mortar", *Proc. Japan Concrete Institute*, **18**(1), 969-974.
Takewaka, K., Yamaguchi, T. and Maeda, S. (2003), "Simulation model for deterioration of concrete structures due to chloride attack", *J. Adv. Concrete Tech.*, **1**(2), 139-146.
Tang, L. and Nilsson, L.O. (1993), "Chloride binding capacity and binding isotherms of OPC pastes and mortars", *Cement Concrete Res.*, **23**(2), 247-253.
Wang, L., Soda, M. and Ueda, T. (2008), "Simulation of chloride diffusivity for cracked concrete based on RBSM and truss network model", *J. Adv. Concrete Tech.*, **6**(1), 143-155.
Xi, Y. and Bazant, Z. (1999), "Modeling chloride penetration in saturated concrete", *J. Mater. Civil Eng.*, **11**(1), 58-65.
Yang, C.C. (2003), "Effect of the interfacial transition zone on the transport and the elastic properties of mortar", *Mag. Concrete Res.*, **55**(4), 305-312.
Yoon, I.S. (2009), "Simple approach to calculate chloride diffusivity of concrete considering carbonation", *Comput. Concrete*, **6**(1), 1-18.

CC

Appendix

Integral of I_1

Generally, one can has the following differential equation

$$\frac{\partial}{\partial x}\left(g_i\frac{\partial C_f}{\partial x}\right)=\frac{\partial g_i}{\partial x}\frac{\partial C_f}{\partial x}+g_i\frac{\partial^2 C_f}{\partial x^2} \tag{A1}$$

It is also like

$$g_i\frac{\partial^2 C_f}{\partial x^2}=\frac{\partial}{\partial x}\left(g_i\frac{\partial C_f}{\partial x}\right)-\frac{\partial g_i}{\partial x}\frac{\partial C_f}{\partial x} \tag{A2}$$

As a result, I_1 will be written as

$$I_1=A\int_{x_i}^{x_j}\left[\frac{\partial}{\partial x}\left(g_i\frac{\partial C_f}{\partial x}\right)-\frac{\partial g_i}{\partial x}\frac{\partial C_f}{\partial x}\right]dx \tag{A3}$$

If set $F(C_f) = C_f$, from Eq. (26) of the text it can be easily obtained as

$$\frac{\partial C_f}{\partial x}=\frac{C_{fj}-C_{fi}}{l} \tag{A4}$$

$$\frac{\partial C_f}{\partial t}=\frac{x_j-x}{l}\frac{\partial C_{fi}}{\partial t}+\frac{x-x_i}{l}\frac{\partial C_{fj}}{\partial t} \tag{A5}$$

Then, by substituting Eq. (A4) into Eq. (A3), it yields

$$I_1=A\left(g_i\frac{\partial C_f}{\partial x}\right)\Bigg|_{x_i}^{x_j}+A\int_{x_i}^{x_j}\frac{1}{l}\left(\frac{C_{fj}-C_{fi}}{l}\right)dx=-A\frac{\partial C_f}{\partial x}\Bigg|_{x=x_i}-\frac{A}{l}(C_{fi}-C_{fj}) \tag{A6}$$

The integral process of I_2 is as follows

$$\begin{aligned}
I_2&=A\int_{x_i}^{x_j}g_i\frac{1}{v(C_f)}\frac{\partial v}{\partial C_f}\left(\frac{\partial C_f}{\partial x}\right)^2dx\\
&=A\int_{x_i}^{x_j}\frac{x_j-x}{l}\frac{\partial C_f}{\partial x}d[\ln v(C_f)]\\
&=A\int_{x_i}^{x_j}\frac{C_{fj}-C_{fi}}{l^2}(x_j-x)d[\ln v(C_f)]\\
&=\frac{A}{l^2}(C_{fj}-C_{fi})\left[(x_j-x)\ln v(C_f)\Big|_{x_i}^{x_j}+\int_{x_i}^{x_j}\ln v(C_f)dx\right]\\
&=\frac{A}{l^2}(C_{fj}-C_{fi})\left[-l\ln v(C_{fi})+\int_{x_i}^{x_j}\left(\frac{x_j-x}{l}\ln v(C_{fi})+\frac{x-x_i}{l}\ln v(C_{fj})\right)dx\right]\\
&=\frac{A}{l^2}(C_{fj}-C_{fi})\left[-l\ln v(C_{fi})+\frac{l}{2}\ln v(C_{fi})+\frac{l}{2}\ln v(C_{fj})\right]\\
&=\frac{A}{2l}(C_{fj}-C_{fi})\ln\frac{v(C_{fj})}{v(C_{fi})}
\end{aligned} \tag{A7}$$

The integral process of I_3 is as follows

$$
\begin{aligned}
I_3 &= -A\int_{x_i}^{x_j} g_i \frac{u(C_f)}{v(C_f)}\frac{\partial C_f}{\partial t}dx \\
&= -A\int_{x_i}^{x_j} \frac{x_j - x}{l}\left[\frac{x_j - x}{l}\frac{u(C_{fi})}{v(C_{fi})}\frac{\partial C_{fi}}{\partial t} + \frac{x - x_i}{l}\frac{u(C_{fj})}{v(C_{fj})}\frac{\partial C_{fj}}{\partial t}\right]dx \\
&= -\frac{A}{l^2}\left[\frac{u(C_{fi})}{v(C_{fi})}\frac{\partial C_{fi}}{\partial t}\int_{x_i}^{x_j}(x_j - x)^2 dx + \frac{u(C_{fj})}{v(C_{fj})}\frac{\partial C_{fj}}{\partial t}\int_{x_i}^{x_j}(x_j - x)(x - x_i)dx\right] \\
&= -\frac{Al}{3}\frac{u(C_{fi})}{v(C_{fi})}\frac{\partial C_{fi}}{\partial t} - \frac{Al}{6}\frac{u(C_{fj})}{v(C_{fj})}\frac{\partial C_{fj}}{\partial t}
\end{aligned}
\tag{A8}
$$

With the similar procedure, J_1, J_2 and J_3 can be obtained as follows

$$
J_1 = A\left.\frac{\partial C_f}{\partial x}\right|_{x = x_j} - \frac{A}{l}(-C_{fi} + C_{fj}) \tag{A9}
$$

$$
J_2 = \frac{A}{2l}(C_{fj} - C_{fi})\ln\frac{v(C_{fj})}{v(C_{fi})} \tag{A10}
$$

$$
J_3 = -\frac{Al}{6}\frac{u(C_{fi})}{v(C_{fi})}\frac{\partial C_{fi}}{\partial t} - \frac{Al}{3}\frac{u(C_{fj})}{v(C_{fj})}\frac{\partial C_{fj}}{\partial t} \tag{A11}
$$